

Synthesis of a pH-responsive functional covalent organic framework via facile and rapid one-step post-synthetic modification and its application in highly efficient *N*-methyladenosine extraction

Yu-Fang Ma, Fang Yuan, Yue Yu, Ying-Lin Zhou, and Xin-Xiang Zhang

Anal. Chem., **Just Accepted Manuscript** • DOI: 10.1021/acs.analchem.9b04600 • Publication Date (Web): 08 Dec 2019

Downloaded from pubs.acs.org on December 8, 2019

Just Accepted

“Just Accepted” manuscripts have been peer-reviewed and accepted for publication. They are posted online prior to technical editing, formatting for publication and author proofing. The American Chemical Society provides “Just Accepted” as a service to the research community to expedite the dissemination of scientific material as soon as possible after acceptance. “Just Accepted” manuscripts appear in full in PDF format accompanied by an HTML abstract. “Just Accepted” manuscripts have been fully peer reviewed, but should not be considered the official version of record. They are citable by the Digital Object Identifier (DOI®). “Just Accepted” is an optional service offered to authors. Therefore, the “Just Accepted” Web site may not include all articles that will be published in the journal. After a manuscript is technically edited and formatted, it will be removed from the “Just Accepted” Web site and published as an ASAP article. Note that technical editing may introduce minor changes to the manuscript text and/or graphics which could affect content, and all legal disclaimers and ethical guidelines that apply to the journal pertain. ACS cannot be held responsible for errors or consequences arising from the use of information contained in these “Just Accepted” manuscripts.

Synthesis of a pH-responsive functional covalent organic framework *via* facile and rapid one-step post-synthetic modification and its application in highly efficient *N*¹-methyladenosine extraction

Yu-Fang Ma, Fang Yuan, Yue Yu, Ying-Lin Zhou* and Xin-Xiang Zhang*

Beijing National Laboratory for Molecular Sciences (BNLMS), MOE Key Laboratory of Bioorganic Chemistry and Molecular Engineering, College of Chemistry and Molecular Engineering, Peking University, Beijing 100871, China.

ABSTRACT: A facile and rapid post-synthetic modification strategy for functionalization of covalent organic framework (COF) was developed to synthesize a tailor-made pH-responsive COF called TpPa-1@Au@GSH for highly efficient extraction of *N*¹-methyladenosine (*m*¹A). Glutathione (GSH) was judiciously designed as the functional group for extracting and releasing *m*¹A by pH variations. With the aid of gold nanoparticles (Au NPs) as linkers, GSH was successfully introduced to the robust substrate TpPa-1 in only one step spending only one hour. Owing to the several-to-one immobilization of GSH on Au NPs, and the large surface area of TpPa-1, this functional COF was constructed with abundant *m*¹A binding sites. TpPa-1@Au@GSH showed excellent selectivity for *m*¹A extraction by capturing *m*¹A from a mixture of 14 nucleoside analogues followed by the mass spectrometry analysis. And it was proved to have ultra-fast adsorption ability (only 1 min incubation time), high binding capacity (5 mg g⁻¹, *m*¹A /TpPa-1@Au@GSH), good reusability (at least 5 times) and good storage stability (at least 8 months at room temperature). Great performance was also achieved in extracting *m*¹A from both animal and plant biological samples. The adsorption mechanism was demonstrated to be based on the electrostatic interaction. This work proposed a new approach for *m*¹A extraction, demonstrated the high potential of COFs in biological sample pretreatment, and offered an effective and versatile route for functionalization of COFs.

*N*¹-methyladenosine (*m*¹A), a prevalent RNA post-transcriptional modification bearing a positively charged base, has been found to be dynamic and reversible in mRNA^{1,2} and participate in many significant biological events³⁻⁵. These exciting achievements attract increasing interest from scientific researchers and encourage them to make more attempts to discover other biological functions of *m*¹A and its role in clinical diagnoses. On account of the particular chemical structure, *m*¹A can undergo Dimroth rearrangement to *m*⁶A in alkaline environment,⁶ which emphasizes the importance of condition control during the measurement of *m*¹A.

To date, mass spectrometry (MS) has been universally used for nucleoside detection due to its great detection sensitivity and qualitative ability.^{7,8} Before MS analyses, removing the impurities, which may cause MS ionization source contamination and signal suppression of target compounds, is quite necessary. Several materials have been developed for nucleoside isolation and purification. The most often used ones are boronate affinity materials,^{9,10} which can capture and release *cis*-diol-containing targets by changing pH from basic to acidic, and polymeric reverse-phase materials,^{11,12} which extract nucleosides based on the hydrophobicity and hydrophilicity. But these aforementioned materials are not such suitable for highly efficient extraction of *m*¹A because of the ionic characteristic of *m*¹A and its instability in alkaline conditions. New approaches based on other mechanisms should be proposed for *m*¹A extraction.

Covalent organic frameworks (COFs) are an emerging class of crystalline porous materials, whose backbone is entirely made up of light elements.^{13,14} Diverse organic building blocks with rigid conformation are linked by strong covalent bonds and

precisely integrated into periodic networks. Owing to their intriguing properties, including low mass density, large surface area, high thermal and chemical stability, highly ordered pore structures, tunable pore size and very flexible molecular design, COFs are well known for their applications in gas adsorption and storage,¹⁵⁻¹⁷ catalysis,^{18,19} optoelectronics,^{20,21} separation,^{22,23} etc. With the aim of making COFs appropriate for further advanced functions and enhancing their application efficiency, functionalization of COFs has gained great concern and developed rapidly. Until now, taking advantage of the highly flexible designability, various functional COFs have been constructed for specific applications, such as detection and removal of heavy metal ions,^{24,25} sample pretreatment²⁶ and chiral separation²⁷, by modifying tailored functional groups.

Generally, approaches for functionalization of COFs can be summarized as two strategies, post-synthetic modification²⁸⁻³¹ and bottom-up strategy³². Compared with the bottom-up strategy, post-synthetic modification is much easier and more popular without the trouble both in the design of functional building blocks, which must follow the principles of constructing a crystalline and ordered COF, and in the complicated condition optimizations for the syntheses of COFs. However, in post-synthetic modification, complex reaction steps and violent reaction conditions typically increase the risk of skeleton decomposition of COFs. And difficult experiment operation always appears as a setback for the further use of a reaction. Thus, facial post-synthetic modification methods are highly desired for the construction of functional COFs.

Inspired by the functionalization of COFs for specific applications, the selective extraction of *m*¹A was anticipated to be

achieved by newly functionalized COFs designed with particular functional groups. Herein, a tailor-made functional COF called TpPa-1@Au@GSH was synthesized for highly efficient extraction of m^1A . And a facile and rapid post-synthetic modification strategy was developed for functionalization of COFs. Considering the uniquely intrinsic positive charge on m^1A and the rigorous demand for pH control, a pH-sensitive tripeptide glutathione (GSH), which could adopt negative charge state under neutral condition and adopt neutral or even positive charge state under acidic condition was chosen as the functional group for selectively adsorbing and releasing m^1A . In order to functionalize the stable porous substrate TpPa-1 with GSH, a one-step functionalization strategy based on gold nanoparticles (Au NPs) was developed. Utilizing the immobilization of GSH on Au NPs and the formation and dispersion of Au NPs on TpPa-1, Au NPs were judiciously designed as bridges that linked GSH and TpPa-1 together. And Au NPs made a great contribution to the increase of functional group density by allowing several GSH molecules to assemble on one gold nanoparticle surface. The functionalization was successfully achieved by a one-step reaction lasting only one hour. For m^1A extraction, this material exhibited excellent selectivity, ultra-rapid capture ability, high binding capacity, good reusability and storage stability. And we demonstrated the adsorption mechanism was based on the electrostatic interaction between TpPa-1@Au@GSH and m^1A . Additionally, this material was successfully applied to the extraction of m^1A from complex biological samples followed by the mass spectrometry analyses.

EXPERIMENTAL SECTION

Reagents. N^1 -methyladenosine was purchased from Berry & Associates (MI, USA). Inosine (I), adenosine (A), cytidine (C) and 5-methylcytidine (m^5C) were purchased from J&K Scientific Ltd (Beijing, China). Guanosine (G), uridine (U) and 2'-O-methyladenosine (Am) were purchased from Shanghai Yuanye Biological Technology Co. Ltd (Shanghai, China). 2'-O-methylguanosine (Gm) and 2'-O-methylcytidine (Cm) were purchased from Aladdin Chemistry Co. Ltd (Shanghai, China). 2'-O-methyluridine (Um) was purchased from Dalian Meilun Biotechnology Co. Ltd (Dalian, China). N^6 -methyladenosine (m^6A) was purchased from Shanghai Macklin Biochemical Co. Ltd (Shanghai, China). Pseudouridine (Ψ) and 5-hydroxymethylcytidine (hm^5C) were purchased from Toronto Research Chemicals (ON, Canada). Formic acid (FA) was purchased from Tokyo Chemical Industry Co. Ltd (Tokyo, Japan). Glutathione, trifluoroacetic acid (TFA) and ammonia solution were purchased from Aladdin Chemistry Co. Ltd (Shanghai, China). *N,N*-Dimethylformamide, HCl and magnesium sulfate were purchased from Xilong Scientific Co. Ltd (Guangdong, China). $CDCl_3$, tetramethylsilane (TMS) and adamantane were purchased from J&K Scientific Ltd (Beijing, China). Paraphenylenediamine (Pa-1), dried phloroglucinol and chloroauric acid ($HAuCl_4 \cdot 4H_2O$) were purchased from Sinopharm Chemical Reagent Co. Ltd (Beijing, China). Hexamethylenetetramine (HMTA), sodium borohydride ($NaBH_4$), sodium chloride (NaCl), sodium hydroxide (NaOH), ethanol and dichloromethane were purchased from Beijing Tong Guang Fine Chemicals Company (Beijing, China). Acetic acid (CH_3COOH) was purchased from Alfa Aesar (MA, USA). Methanol (LC-MS Grade) was purchased from J.T.Baker (WI, USA). Water used in this work was purified using a Milli-Q water purification system (Millipore). All materials and reagents were at least of analytical grade and used without further purification.

Synthesis of TpPa-1@Au@GSH. 1, 3, 5-Tri-formylphloroglucinol (Tp) was synthesized according to Chong *et al.*³³ TFA (60 mL) was added to a mixture of HMTA (10.065 g) and dried phloroglucinol (4.009 g). And the solution was heated at 100 °C for 2.5 h under nitrogen atmosphere. HCl (3 M in H_2O , 100 mL) was added afterwards and heated at 100 °C for 1 h under nitrogen atmosphere. After cooling to room temperature, the solution was filtered, extracted with dichloromethane (250 mL), dried over magnesium sulfate and concentrated by rotary evaporation. The obtained solid was washed with ethanol and dried under vacuum to give an off-white powder.

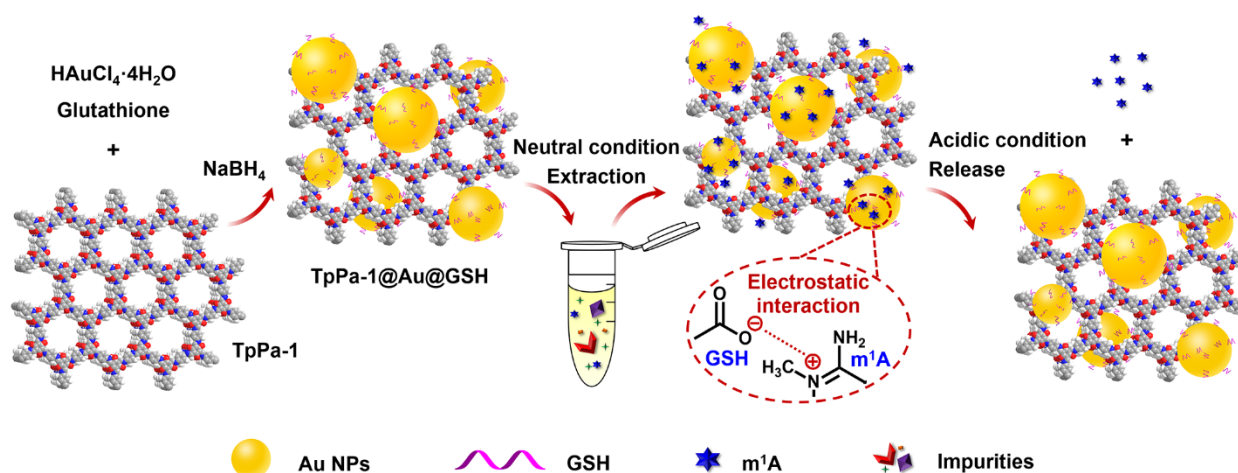
TpPa-1 was synthesized according to Kandambeth *et al* with a few modifications.³⁴ Tp (25.2 mg) and Pa-1 (19.2 mg) were added to ethanol (8 mL) respectively. After being sonicated for about 10 minutes, Tp and Pa-1 were mixed sufficiently in a Teflon autoclave. The Teflon autoclave was replenished with nitrogen, sealed off and heated at 90 °C for 24 h. The obtained powder was then solvent exchanged with *N,N*-dimethylformamide and ethanol successively and dried under vacuum to give a deep red powder.

TpPa-1@Au@GSH was synthesized by a one-step post-synthetic modification of TpPa-1. A well-dispersed suspension of TpPa-1 (80 mg) and $HAuCl_4 \cdot 4H_2O$ solution (10 mg mL^{-1} in H_2O , 8 mL) was added with GSH solution (40 mg mL^{-1} in H_2O , 8 mL). The pH of the mixture was adjusted to 5 using NaOH solution (1 M in H_2O). A $NaBH_4$ solution (150 mM in H_2O , 12 mL) was then added and the suspension was stirred in the dark at room temperature for 1 hour. The collected mixture was filtered, washed with plenty of water and finally dried to give a dark red powder.

For the comparison of the m^1A extraction ability between different materials, TpPa-1@Au was synthesized. The synthesis process was as follows. TpPa-1 (1 mg) was dispersed in H_2O (190 μL) and mixed with $HAuCl_4 \cdot 4H_2O$ solution (100 mg mL^{-1} in H_2O , 10 μL). The suspension was stirred in an ice bath for 1 hour. A $NaBH_4$ solution (150 mM in H_2O , 50 μL) was then added and the mixture was stirred in the ice bath for 30 minutes. The obtained suspension was filtered and washed with water. And a dark red powder was obtained after dried under vacuum.

Characterization. 1H nuclear magnetic resonance (1H NMR) and ^{13}C nuclear magnetic resonance (^{13}C NMR) spectra were obtained on a Bruker Avance 500 spectrometer and were referenced to TMS and $CDCl_3$, respectively. ^{13}C cross-polarization total suppression of sidebands magic-angle-spinning (CP-TOSS MAS) solid-state NMR spectra were carried out on a Bruker Avance 400 spectrometer and were referenced to adamantane. Fourier transform infrared (FT-IR) spectra were recorded on a Bruker Tensor 27 spectrometer. Transmission electron microscopy (TEM) images were recorded on a JEOL JEM-2100F microscope at 200 kV. The X-ray diffraction (XRD) patterns were recorded on a Phillips PANalytical X'pert pro diffractometer using $Cu K\alpha$ radiation ($\lambda=1.54 \text{ \AA}$). The scan rate was set as 1° min^{-1} and the step size was 0.02° . Zeta potential analyses were carried out on a Brookhaven ZetaPlus instrument. Scanning electron microscopy-energy dispersive spectroscopy (SEM-EDS) analysis was carried out on a Hitachi S-4800 scanning electron microscope equipped with an Ametek Apollo XP EDS detector. Thermogravimetric analyses (TGA) were performed on a Mettler Toledo TGA/DSC 1 analyzer.

Selective Extraction of m^1A . Four basic nucleosides (A, U, C, G) and ten modified nucleosides (m^1A , m^6A , Am, I, Gm, Um,

Scheme 1. One-step post-synthetic modification of TpPa-1 and selective extraction and release of m¹A using TpPa-1@Au@GSH.

Ψ, Cm, m⁵C, hm⁵C) were prepared as the standard solutions at 10 nM (in H₂O) respectively. For the evaluation of selectivity, these fourteen nucleosides (30 μL for each) were mixed to form the loading solution and treated with TpPa-1@Au@GSH. In detail, TpPa-1@Au@GSH (1 mg) was dispersed sufficiently in the standard solution and incubated with it for the capture of m¹A. Afterwards, a centrifugation step was carried out to separate TpPa-1@Au@GSH from the solution. Impurities remained on the material caused by the non-specific adsorption were removed using washing buffer (H₂O). And the captured m¹A was released by a plenty of H₂O containing 2% CH₃COOH (v/v), which was used as the elution buffer. The collected eluate was lyophilized and redissolved in H₂O (30 μL) followed by the LC-MS/MS analysis.

For optimization of extraction conditions and comparison of different materials, mixtures of seven nucleosides, including four basic nucleosides (A, U, C, G) and three modified nucleosides (m¹A, m⁶A, Am) generated from adenosine, were used for the extraction. And the investigations on capacity, reusability, storage stability and adsorption mechanism were carried out with m¹A standard solution. The adsorption mechanism was demonstrated by changing the pH values and ionic strength of standard solution and washing buffer. Here, the pH values were adjusted by ammonia solution and CH₃COOH aqueous solution (pH=3, 5, 7, 8, 9, 11), and the ionic strength was changed by varying the NaCl concentrations of the standard solution and washing buffer (concentrations of NaCl=0 mM, 5 mM, 10 mM, 50 mM).

Extraction of m¹A from biological samples were performed with mouse serum and stems and roots of *Arabidopsis thaliana*. Mouse serum was collected from a healthy mouse, diluted with H₂O and directly used for further extraction. *Arabidopsis thaliana* was collected from a growth chamber. After being washed with ultrapure water, the stems or roots were cut off, snap frozen in liquid nitrogen and immediately ground into powder. Subsequently, H₂O was added to obtain all the water-soluble molecules from the powder sample. And the supernatant was separated from the residues and collected for extraction. The extraction process was the same as above. Briefly, prepared biological sample (50 μL) was mixed with TpPa-1@Au@GSH followed by the removal of impurities and release of captured m¹A. The obtained eluate was lyophilized and redissolved in H₂O (50 μL) for LC-MS/MS analysis. The extraction recovery

of each biological sample was calculated by standard addition test.

LC-MS/MS Analysis. LC-MS/MS analyses were performed on a Thermo Scientific Dionex Ultimate 3000 HPLC system connected to a Triple Quad™ 5500 mass spectrometer equipped with an electrospray ion source. A C18 column (2.1 mm × 100 mm, 1.8 μm) was used for sample separation with a flow rate of 0.3 mL min⁻¹ at 35 °C. 0.0085% FA in water (v/v) and 0.0085% FA in MeOH were prepared as mobile phase A and mobile phase B, respectively. The separation gradient was as follows: 100% A for 2 min, 100–95% A for 6 min, 95–20% A for 0.1 min, 20–0% A for 1.9 min and 0% A for 1 min.

The mass spectrometry detection was performed under positive ion mode with multiple reaction monitoring (MRM). The MRM parameters of nucleosides were listed in Table S1. The MS parameters were set as follows: curtain gas: 20 psi, collision gas: 8 psi, ionspray voltage: 5500 V, ion source gas 1: 65 psi, ion source gas 2: 55 psi, interface heater temperature: 500 °C, declustering potential: 55 V, entrance potential: 10 V and collision cell exit potential: 16 V. MultiQuant 3.0.2 Software was used for the data processing.

RESULTS AND DISCUSSION

Design of TpPa-1@Au@GSH for m¹A Extraction. A functional COF TpPa-1@Au@GSH, which was synthesized by decorating TpPa-1 with Au NPs and GSH, was designed for the selective extraction of m¹A (Scheme 1). The functionalization strategy was designed to be a one-step post-synthetic modification with the assistance of Au NPs. Au NPs might act as satisfactory linkers that connected GSH with the stable substrate TpPa-1. They could load firmly on TpPa-1 with the help of extra interactions offered by the enriched oxygen and nitrogen in reticular TpPa-1 skeleton.^{35,36} And they let GSH assembled on their surfaces *via* strong Au-S bonds. The tripeptide GSH provided not only thiol for the immobilization, but also carboxyl and amino as functional groups for m¹A extraction. The presence of zwitterionic GSH had the potential advantage of making TpPa-1@Au@GSH a pH-responsive material with different charge states under different pH conditions, which was favorable for the extraction and release of the positively charged molecule m¹A. In detail, TpPa-1@Au@GSH served as negative charge provider under neutral condition to capture m¹A, and it changed to be neutral or even positive under acidic condition to free the adsorbed m¹A. It is noteworthy to mention that, this

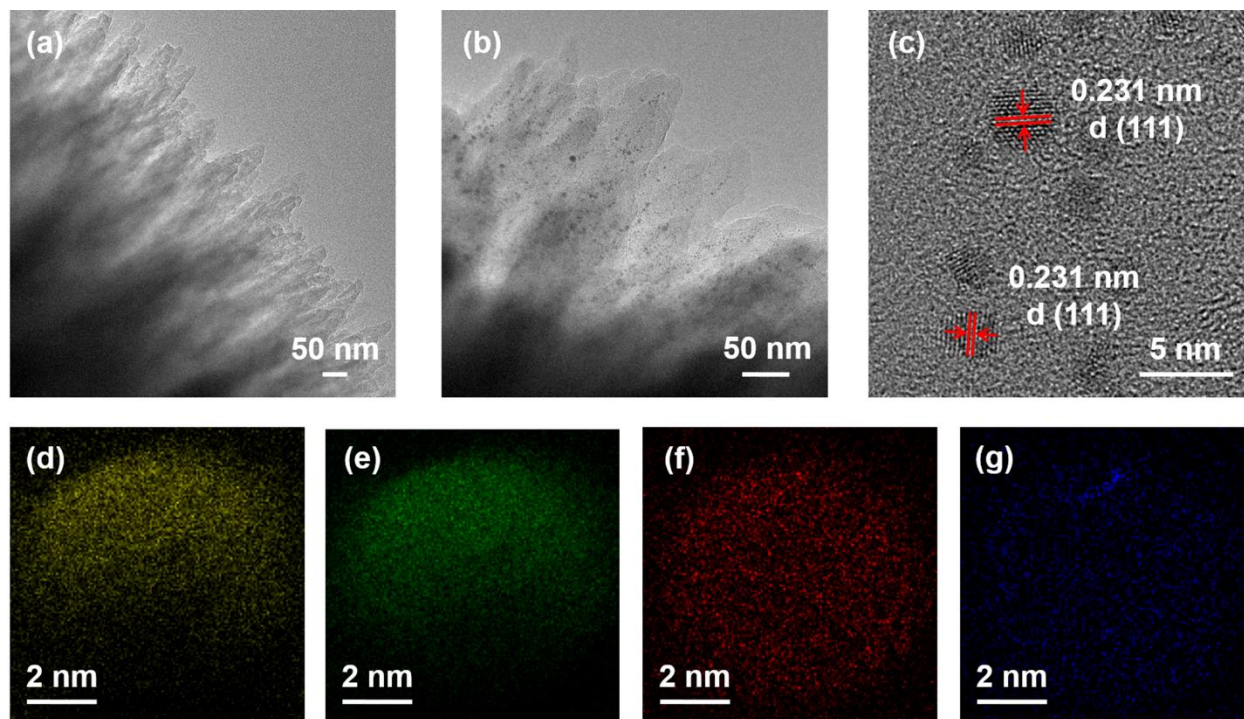


Figure 1. TEM images of (a) TpPa-1 and (b) TpPa-1@Au@GSH. (c) High resolution TEM image of TpPa-1@Au@GSH. SEM-EDS analyses of (d) N, (e) O, (f) S and (g) Au of TpPa-1@Au@GSH.

post-synthetic modification strategy might introduce the functional groups in a several-to-one mode. Porous structure and large surface area of the substrate TpPa-1, provided Au NPs with abundant loading sites for their high dispersion, and avoided the aggregation of these nanoparticles. And several GSH molecules were simultaneously immobilized onto one gold nanoparticle surface. The plenty functional groups on the generated COF were pretty beneficial for its further application in m^1A extraction.

Synthesis and Characterization of TpPa-1@Au@GSH.

Firstly, Tp, one of the organic units for the building of TpPa-1 was synthesized *via* an easy and quick reaction called Duff formylation using phloroglucinol as a precursor. Subsequently, the obtained Tp and Pa-1, another organic unit, carried out the Schiff base reaction and formed the covalent organic framework TpPa-1. For the post-synthetic modification, TpPa-1, HAuCl₄·4H₂O and GSH were mixed together followed by the addition of NaBH₄, a reducing agent for the conversion of gold ions to gold nanoparticles (Scheme 1).

¹H NMR and ¹³C NMR spectra of Tp demonstrated the successful synthesis of this organic building unit (Figure S1). ¹H NMR (500 MHz, CDCl₃, δ): 14.11 (s, 3H, OH), 10.16 (s, 3H, CHO); ¹³C NMR (125 MHz, CDCl₃, δ): 192.08 (CHO), 173.61 (COH), 102.90 (CCHO). And it was also verified by the FT-IR analysis (Figure S2). Compared with the FT-IR spectra of Tp and Pa-1, spectrum of TpPa-1 indicated the complete consumption of the reactants and the existence of the newly formed keto tautomer (Figure S2). The XRD pattern of TpPa-1 revealed the good crystallinity of the obtained COF by the appearance of peaks at $2\theta=4.7, 8.3, 11.1, \text{ and } 27^\circ$ (Figure S3).

To verify the loading of Au NPs on substrate TpPa-1, TEM analyses of TpPa-1 and TpPa-1@Au@GSH were firstly carried out (Figure 1a, b and c). After the modification, abundant Au NPs were observed on TpPa-1@Au@GSH. The Au NPs were

highly dispersed without aggregation. And by the high resolution TEM analysis of TpPa-1@Au@GSH, the formation of Au NPs oriented in the (111) plane with an interplanar *d*-spacing of 0.231 nm was demonstrated. Compared with TpPa-1, the XRD pattern of TpPa-1@Au@GSH with additional peaks appearing at the range of $2\theta=35^\circ\text{--}85^\circ$, which corresponding with the Au NPs, also verified the loading of Au NPs (Figure S3). Moreover, the XRD patterns revealed the retained integrity of TpPa-1 with slight loss of crystallinity after the functionalization. It revealed that TpPa-1 was stable enough under this functionalization condition and was a suitable substrate. SEM-EDS analysis of TpPa-1@Au@GSH was performed to demonstrate the assembling of GSH on Au NPs (Figure 1d, e, f and g). The simultaneously appearance of N, O, Au and S element signals on the material indicated not only the loading of Au NPs on TpPa-1, but also the successful decoration of GSH on Au NPs. Zeta potential analyses, which showed a shift from -14.67 ± 1.47 mV (TpPa-1 in H₂O) to -42.09 ± 1.01 mV (TpPa-1@Au@GSH in H₂O), also provided an evidence for the immobilization of GSH on Au NPs. We evaluated the thermal stability of TpPa-1@Au@GSH and found a slightly weight loss at relatively low temperature (Figure S4). This weight loss might be due to the decomposition of modified GSH. And in comparison with TpPa-1, TGA curve of TpPa-1@Au@GSH showed the retention of the thermal stability of TpPa-1, which emphasized the superiority of TpPa-1 as a functionalization substrate. We also carried out the FT-IR (Figure S2) and ¹³C CP-TOSS MAS solid-state NMR analyses (Figure S5) of TpPa-1@Au@GSH. And the results showed that the TpPa-1 framework remained intact even after the treatment with NaBH₄, which indicated the great stability of this robust substrate again.

As we can see, the functionalization reaction contained only one step and was rapidly accomplished in only one hour. Compared with most of the post-synthetic modification strategies developed for functionalization of COFs,³⁷⁻⁴¹ this strategy was

less time-consuming and more facile. Moreover, this modification was performed in water without any organic solvent, which was safe to operate and environmentally friendly.

Evaluations of TpPa-1@Au@GSH for the Selective Extraction of m¹A. The obtained functional COF TpPa-1@Au@GSH was applied to the selective extraction of m¹A (Scheme 1). The procedure of extraction contained three steps, loading, washing and elution, which were used for capture of m¹A, removal of non-specific adsorbed impurities and release of m¹A, respectively. In order to reach the best performance, the extraction conditions were optimized carefully. The composition of the loading buffer as well as washing buffer was optimized by varying the ratio of MeOH to H₂O (Figure S6). Buffers without MeOH gave the best efficiency and was used for the following experiments. For the optimization of incubation time (Figure 2a), we surprisingly found that, only 1 min was enough for TpPa-1@Au@GSH to capture m¹A without any loss in selectivity. The ultra-rapid capture ability was very advantageous for the extraction process with less time consumption. And we attributed this outstanding property to the high affinity offered by abundant GSH.

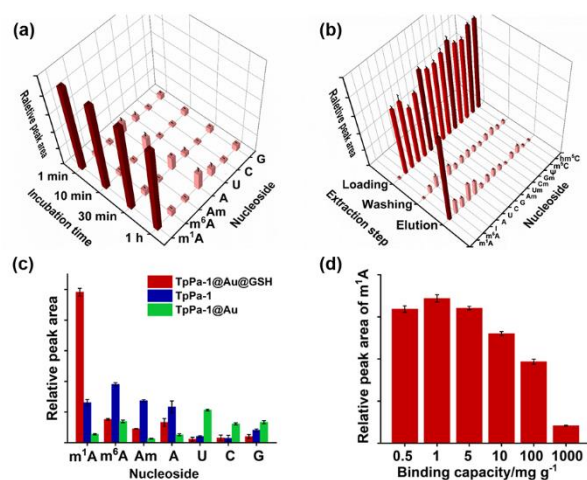


Figure 2. Evaluations of the method and material. (a) Performance of m¹A extraction by TpPa-1@Au@GSH with different incubation time. (b) Selective extraction of m¹A from a mixture of 14 nucleoside analogues by TpPa-1@Au@GSH. (c) Comparison of the performance of m¹A extraction by different materials. (d) Evaluation of the binding capacity (m¹A/TpPa-1@Au@GSH) of TpPa-1@Au@GSH. In figure (a) and (b), for each nucleoside, the z axis=peak area of detected nucleoside/peak area of this nucleoside before extraction. Color from deep to light represents the number from large to small. In figure (c), for each nucleoside, the y axis=peak area of detected nucleoside/peak area of this nucleoside before extraction. In figure (d), the y axis represents the peak area of m¹A compared with other groups. The error bars represent the standard deviations of three parallel tests.

To evaluate the extraction selectivity, 13 nucleoside analogues were chosen as interfering molecules and mixed with m¹A followed by the adsorption using TpPa-1@Au@GSH. As shown in Figure 2b, except m¹A, the other nucleosides could hardly be adsorbed by TpPa-1@Au@GSH and were left in loading buffer. In contrast, there was almost no m¹A in loading and washing buffer. The vast majority of m¹A was efficiently extracted and subsequently released in the elution step. It showed that, although as many as 13 analogues existed in the solution, TpPa-1@Au@GSH had the ability to adsorb m¹A

with remarkable selectivity. Compared this material with the substrate TpPa-1 (Figure 2c), TpPa-1@Au@GSH showed excellent selectivity to m¹A, while TpPa-1 failed to extract the target from the solution. TpPa-1@Au was also applied to the extraction, and little m¹A was eluted from the material (Figure 2c). These results indicated the extremely essential role of GSH in the extraction and highlighted the importance of the functionalization.

Binding capacity of TpPa-1@Au@GSH was explored by applying different amounts of materials to extract the same amount of m¹A (Figure 2d). The peak area of extracted m¹A was used as indicators to judge whether TpPa-1@Au@GSH was overloaded. Benefiting from the low mass density and porous architecture of TpPa-1, abundant binding sites, and high affinity to m¹A, the maximum binding capacity of this material was estimated to be as high as 5 mg g⁻¹ (m¹A/TpPa-1@Au@GSH).

The reusability and the storage stability of TpPa-1@Au@GSH were also investigated. According to the results (Figure S7 and S8), no distinct change was observed in m¹A extraction efficiency even after 5 repeated use or after 8 months storage, demonstrating the good stability of this material under the extraction conditions and its good storage stability at room temperature.

Investigation of the Adsorption Mechanism. Considering the zwitterionic groups in GSH and the positive charge in m¹A, the adsorption mechanism was supposed to be based on the electrostatic interaction. To verify this hypothesis, the following investigations were carried out.

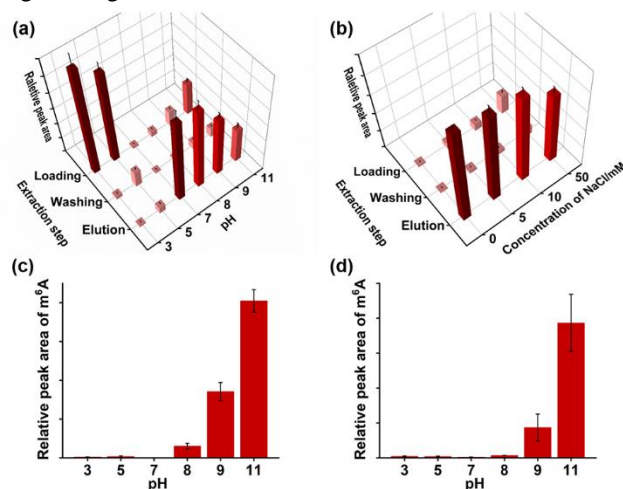


Figure 3. Investigation of the adsorption mechanism. (a) Effect of pH on the adsorption of m¹A. (b) Effect of ionic strength on the adsorption of m¹A. m⁶A rearranged from m¹A in (c) loading buffer and (d) washing buffer under different pH values. In figure (a) and (b), for each group, the z axis=peak area of detected m¹A/peak area of m¹A before extraction. Color from deep to light represents the number from large to small. In figure (c) and (d), the y axis represents the peak area of m⁶A compared with other groups. The error bars represent the standard deviations of three parallel tests.

On account of the different ionization forms of GSH under different pH, the pH values of loading buffer as well as washing buffer were adjusted from 3 to 11. And the obtained buffers were applied to the m¹A extraction to explore the influences caused by various pH. As shown in Figure 3a, the best adsorption efficiency of TpPa-1@Au@GSH appeared at pH=7, and

the efficiency sharply declined at lower pH values. In terms of the pK_a of GSH, GSH was negatively charged under neutral condition. And as the acidity of the condition increased, GSH changed to be electrically neutral or even positively charged. Taking the positive charge in m^1A into consideration, the experiment results were exactly in accord with our hypothesis. In addition, the zeta potential of TpPa-1@Au@GSH under neutral and acidic condition was analyzed respectively. And the results turned out to be -42.09 ± 1.01 mV in water (loading and washing buffer) and 10.24 ± 1.51 mV in H_2O containing 2% CH_3COOH (v/v) (elution buffer), which further verified our hypothesis. And it also demonstrated the pH response ability of our material, which played an extremely vital role in selective extraction and release of m^1A . Notably, although the adsorption efficiency was theoretically considered to be better under alkaline conditions, rearrangement of m^1A to m^6A limited the usage of alkaline buffers (Figure 3c and d).

To strengthen the support of our hypothesis, the m^1A extraction efficiency under different ionic strength of loading and washing buffer, which significantly influenced the electrostatic interaction, was also investigated. As expected, the adsorption of m^1A was interfered by the added ions (Figure 3b). TpPa-1@Au@GSH performed the best in H_2O . Based on the above results, the adsorption affinity between TpPa-1@Au@GSH and m^1A was confirmed to be the electrostatic interaction.

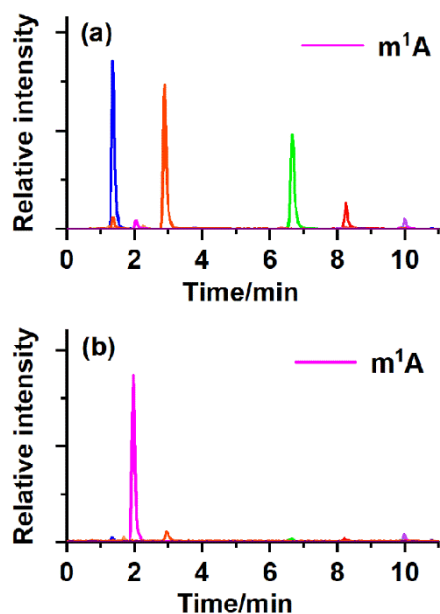


Figure 4. LC-MS chromatographs of *Arabidopsis thaliana* stems (a) without extraction and (b) with extraction using TpPa-1@Au@GSH.

Selective Extraction of m^1A from Complex Biological Samples. *Arabidopsis thaliana* and mouse were widely used as biological models for the exploration of various biological events. We applied TpPa-1@Au@GSH to stems and roots of *Arabidopsis thaliana* and mouse serum to investigate whether this material worked on the m^1A extraction of complex samples. The results of stems were shown in Figure 4. With the aid of TpPa-1@Au@GSH, signal of m^1A dominated the MS spectrum, while others were efficiently eliminated. The applications in roots and mouse serum were also accomplished with excellent

efficiency (Figure S9 and S10). In addition, the extraction recovery of stems, roots and mouse serum was calculated to be $86.9 \pm 2.1\%$, $89.0 \pm 2.8\%$ and $88.1 \pm 1.8\%$, respectively. The remarkable performance of TpPa-1@Au@GSH indicated its high potential in m^1A extraction from both plant and animal biological samples to reveal the biological roles of m^1A .

CONCLUSIONS

In summary, we successfully designed and synthesized a pH-responsive functional COF called TpPa-1@Au@GSH via a one-step post-synthetic modification strategy. And a new approach was proposed for m^1A extraction using this material. Utilizing the intriguing advantages of covalent organic framework TpPa-1 and the abundant incorporation of GSH, TpPa-1@Au@GSH possessed outstanding m^1A extraction ability. In this functionalization strategy, desired functional group GSH was modified on TpPa-1 facily and rapidly by the judiciously addition of gold nanoparticles, which linked GSH to the substrate. We anticipated other thiol-contained functional groups, which were tailored for other specific applications, could also be decorated to the substrate utilizing Au NPs as the intermedia. The post-synthetic modification strategy was predicted to be a promising and versatile access to obtain other functional COFs for further advanced applications.

ASSOCIATED CONTENT

Supporting Information

The Supporting Information is available free of charge on the ACS Publications website.

MRM parameters of the nucleosides, NMR spectra, FT-IR spectra, XRD patterns, TGA data, optimization of the composition of loading buffer as well as washing buffer, reusability and storage stability of TpPa-1@Au@GSH, and selective extraction of m^1A from roots of *Arabidopsis thaliana* and mouse serum (PDF).

AUTHOR INFORMATION

Corresponding Author

*E-mail: zhouyl@pku.edu.cn, zxx@pku.edu.cn; Fax: +86-10-62754112; Tel: +86-10-62754112.

ORCID

Ying-Lin Zhou: 0000-0002-7785-3250

Notes

The authors declare no competing financial interest.

ACKNOWLEDGMENT

This work was supported by the National Natural Science Foundation of China (No. 21575005, 21675004 and 21775006). We thank Dr. Hui Fu for the ^{13}C CP-TOSS MAS solid-state NMR analyses.

REFERENCES

- (1) Dominissini, D.; Nachtergaele, S.; Moshitch-Moshkovitz, S.; Peer, E.; Kol, N.; Ben-Haim, M. S.; Dai, Q.; Di Segni, A.; Salmon-Divon, M.; Clark, W. C.; Zheng, G.; Pan, T.; Solomon, O.; Eyal, E.; Hershkovitz, V.; Han, D.; Dore, L. C.; Amariglio, N.; Rechavi, G.; He, C. *Nature* **2016**, *530*, 441-446.
- (2) Li, X.; Xiong, X.; Wang, K.; Wang, L.; Shu, X.; Ma, S.; Yi, C. *Nat Chem Biol* **2016**, *12*, 311-316.

- (3) Roundtree, I. A.; Evans, M. E.; Pan, T.; He, C. *Cell* **2017**, *169*, 1187-1200.
- (4) Zhang, C.; Jia, G. *Genomics Proteomics Bioinformatics* **2018**, *16*, 155-161.
- (5) Xiong, X.; Li, X.; Yi, C. *Curr Opin Chem Biol* **2018**, *45*, 179-186.
- (6) Macon, J. B.; Wolfenden, R. *Biochemistry* **1968**, *7*, 3453-3458.
- (7) Dudley, E.; Bond, L. *Mass Spectrom Rev* **2014**, *33*, 302-331.
- (8) Banoub, J. H.; Newton, R. P.; Esmans, E.; Ewing, D. F.; Mackenzie, G. *Chemical Reviews* **2005**, *105*, 1869-1915.
- (9) Struck, W.; Siluk, D.; Yumba-Mpanga, A.; Markuszewski, M.; Kaliszán, R.; Markuszewski, M. *J Chromatogr A* **2013**, *1283*, 122-131.
- (10) Jiang, Y.; Ma, Y. *Analytical Chemistry* **2009**, *81*, 6474-6480.
- (11) Yin, R.; Mo, J.; Lu, M.; Wang, H. *Anal Chem* **2015**, *87*, 1846-1852.
- (12) He, L.; Wei, X.; Ma, X.; Yin, X.; Song, M.; Donninger, H.; Yaddanapudi, K.; McClain, C. J.; Zhang, X. *J Am Soc Mass Spectrom* **2019**, *30*, 987-1000.
- (13) Feng, X.; Ding, X.; Jiang, D. *Chem Soc Rev* **2012**, *41*, 6010-6022.
- (14) Ding, S. Y.; Wang, W. *Chem Soc Rev* **2013**, *42*, 548-568.
- (15) Choi, Y. J.; Choi, J. H.; Choi, K. M.; Kang, J. K. *J Mater. Chem.* **2011**, *21*, 1073-1078.
- (16) Doonan, C. J.; Tranchemontagne, D. J.; Glover, T. G.; Hunt, J. R.; Yaghi, O. M. *Nat Chem* **2010**, *2*, 235-238.
- (17) El-Mahdy, A. F. M.; Kuo, C.-H.; Alshehri, A.; Young, C.; Yamauchi, Y.; Kim, J.; Kuo, S.-W. *Journal of Materials Chemistry A* **2018**, *6*, 19532-19541.
- (18) Ding, S. Y.; Gao, J.; Wang, Q.; Zhang, Y.; Song, W. G.; Su, C. Y.; Wang, W. *J Am Chem Soc* **2011**, *133*, 19816-19822.
- (19) Fang, Q.; Gu, S.; Zheng, J.; Zhuang, Z.; Qiu, S.; Yan, Y. *Angew Chem Int Ed Engl* **2014**, *53*, 2878-2882.
- (20) Dogru, M.; Handloser, M.; Auras, F.; Kunz, T.; Medina, D.; Hartschuh, A.; Knochel, P.; Bein, T. *Angew Chem Int Ed Engl* **2013**, *52*, 2920-2924.
- (21) Feng, X.; Chen, L.; Honsho, Y.; Saengsawang, O.; Liu, L.; Wang, L.; Saeki, A.; Irle, S.; Seki, S.; Dong, Y.; Jiang, D. *Adv Mater* **2012**, *24*, 3026-3031.
- (22) Yang, C. X.; Liu, C.; Cao, Y. M.; Yan, X. P. *Chem Commun (Camb)* **2015**, *51*, 12254-12257.
- (23) Oh, H.; Kalidindi, S. B.; Um, Y.; Bureekaew, S.; Schmid, R.; Fischer, R. A.; Hirscher, M. *Angew Chem Int Ed Engl* **2013**, *52*, 13219-13222.
- (24) Ding, S. Y.; Dong, M.; Wang, Y. W.; Chen, Y. T.; Wang, H. Z.; Su, C. Y.; Wang, W. *J Am Chem Soc* **2016**, *138*, 3031-3037.
- (25) Huang, N.; Zhai, L.; Xu, H.; Jiang, D. *J Am Chem Soc* **2017**, *139*, 2428-2434.
- (26) Ma, Y. F.; Wang, L. J.; Zhou, Y. L.; Zhang, X. X. *Nanoscale* **2019**, *11*, 5526-5534.
- (27) Qian, H. L.; Yang, C. X.; Yan, X. P. *Nat Commun* **2016**, *7*, 12104.
- (28) Xu, H.; Gao, J.; Jiang, D. *Nat Chem* **2015**, *7*, 905-912.
- (29) Bunck, D. N.; Dichtel, W. R. *Chem Commun (Camb)* **2013**, *49*, 2457-2459.
- (30) Lohse, M. S.; Stassin, T.; Naudin, G.; Wuttke, S.; Ameloot, R.; De Vos, D.; Medina, D. D.; Bein, T. *Chemistry of Materials* **2016**, *28*, 626-631.
- (31) Rager, S.; Dogru, M.; Werner, V.; Gavryushin, A.; Gätz, M.; Engelke, H.; Medina, D. D.; Knochel, P.; Bein, T. *CrystEngComm* **2017**, *19*, 4886-4891.
- (32) Wang, L.; Dong, B.; Ge, R.; Jiang, F.; Xiong, J.; Gao, Y.; Xu, J. *Microporous and Mesoporous Materials* **2016**, *224*, 95-99.
- (33) Chong, J. H.; Sauer, M.; Patrick, B. O.; MacLachlan, M. J. *Organic Letters* **2003**, *5*, 3823-3826.
- (34) Kandambeth, S.; Mallick, A.; Lukose, B.; Mane, M. V.; Heine, T.; Banerjee, R. *J Am Chem Soc* **2012**, *134*, 19524-19527.
- (35) Pachfule, P.; Kandambeth, S.; Diaz Diaz, D.; Banerjee, R. *Chem Commun (Camb)* **2014**, *50*, 3169-3172.
- (36) Pachfule, P.; Panda, M. K.; Kandambeth, S.; Shivaprasad, S. M.; D'áz, D. D.; Banerjee, R. *J Mater. Chem. A* **2014**, *2*, 7944-7952.
- (37) Guo, H.; Wang, J.; Fang, Q.; Zhao, Y.; Gu, S.; Zheng, J.; Yan, Y. *CrystEngComm* **2017**, *19*, 4905-4910.
- (38) Lu, S.; Hu, Y.; Wan, S.; McCaffrey, R.; Jin, Y.; Gu, H.; Zhang, W. *J Am Chem Soc* **2017**, *139*, 17082-17088.
- (39) Vardhan, H.; Verma, G.; Ramani, S.; Nafady, A.; Al-Enizi, A. M.; Pan, Y.; Yang, Z.; Yang, H.; Ma, S. *ACS Appl Mater Interfaces* **2019**, *11*, 3070-3079.
- (40) Lu, Q.; Ma, Y.; Li, H.; Guan, X.; Yusran, Y.; Xue, M.; Fang, Q.; Yan, Y.; Qiu, S.; Valtchev, V. *Angew Chem Int Ed Engl* **2018**, *57*, 6042-6048.
- (41) Baldwin, L. A.; Crowe, J. W.; Pyles, D. A.; McGrier, P. L. *J Am Chem Soc* **2016**, *138*, 15134-15137.

For Table of Contents Only

